CHINESE OPTICS LETTERS

Vol. 21, No. 4 | April 2023

Photon pair generation in lithium niobate waveguide periodically poled by femtosecond laser

Fan Dai (戴 凡)[1,†], Qianqian Tian (田倩倩)[1,†], Shuangyin Huang (黄双印)[1], Min Wang (王 敏)[1], Chenghou Tu (涂成厚)[1], Yan Sheng (盛 艳)[2,3*], Yongnan Li (李勇男)[1**], and Hui-Tian Wang (王慧田)[4,5]

[1] Key Laboratory of Weak-Light Nonlinear Photonics and School of Physics, Nankai University, Tianjin 300071, China

[2] Laboratory of Infrared Materials and Devices, Research Institute of Advanced Technologies, Ningbo University, Ningbo 315211, China

[3] Laser Physics Center, Research School of Physics and Engineering, Australian National University, Canberra, ACT 2601, Australia

[4] National Laboratory of Solid State Microstructures, Nanjing University, Nanjing 210093, China

[5] Collaborative Innovation Center of Advanced Microstructures, Nanjing University, Nanjing 210093, China

*Corresponding author: yan.sheng@anu.edu.au

**Corresponding author: liyongnan@nankai.edu.cn

Received October 17, 2022 | Accepted November 25, 2022 | Posted Online April 6, 2023

Reliable generation of single photons is of key importance for fundamental physical experiments and quantum protocols. The periodically poled lithium niobate (LN) waveguide has shown promise for an integrated quantum source due to its large spectral tunability and high efficiency, benefiting from the quasi-phase-matching. Here we demonstrate photon-pair sources based on an LN waveguide periodically poled by a tightly focused femtosecond laser beam. The pair coincidence rate reaches ∼8000 counts per second for average pump power of 3.2 mW (peak power is 2.9 kW). Our results prove the possibility of application of the nonlinear photonics structure fabricated by femtosecond laser to the integrated quantum source. This method can be extended to three-dimensional domain structures, which provide a potential platform for steering the spatial degree of freedom of the entangled two-photon states.

Keywords: photon pair; spontaneous parametric downconversion; femtosecond laser; lithium niobate waveguide; quasi-phase matching.

DOI: 10.3788/COL202321.042701

1. Introduction

Quantum photonic technology exhibits great potential for applications ranging from quantum communications[1–3] and quantum computation[4–6] to quantum metrology[7,8]. In particular, the recent advances in integrated quantum photonics[9–13] have shown great promise for chip-scale quantum information processing with unprecedented capability and complexity. Single-mode, high-purity, and integrated sources of single photons and/or entangled photon pairs are necessary for all these quantum protocols[14–16].

Silicon photonic integration platforms provide third-order nonlinearity $\chi^{(3)}$ that enables photon-pair generation by spontaneous four-wave mixing (SFWM)[17–20]. Its major advantages are natural compatibility with the CMOS industry, and extremely well-developed fabrication techniques for silicon electronics and photonics. Another attractive candidate of the quantum integration platform is optical nonlinear dielectric materials, such as lithium niobate (LN) and potassium titanyl phosphate (KTP)[21–23]. Compared with the third-order nonlinearities $\chi^{(3)}$, photon pairs can be produced through spontaneous parametric downconversion (SPDC) in nonlinear crystals based on the strong second-order nonlinearity $\chi^{(2)}$ that is more efficient and requires lower pump power[24]. More specifically, periodical poling, also known as the ferroelectric domain-engineering technique[25], can be applied to the $\chi^{(2)}$ nonlinear crystal to realize quasi-phase-matching (QPM) SPDC for generation of entangled photons with higher efficiency[26,27]. By using properly designed $\chi^{(2)}$ structures, ultrabroadband entangled photon pairs can be obtained with tunable spectral properties[28,29].

The traditional fabrication method for QPM is electric field poling, but it cannot be used to manipulate $\chi^{(2)}$ along the depth of the medium. The external poling field has to be applied via patterned electrodes on the crystal surface, and the ferroelectric domain switching process always begins with nucleation of inverted domains on the surface. In addition, the mask and lithography are needed to design the poling structure, which are feasible but not ideal for rapid prototyping. Recently, the

fabrication of QPM structures in ferroelectrics using femtosecond lasers has been reported[30–34]. The laser beam can be focused at multiple depths inside a transparent medium for fabrication of three-dimensional (3D) nonlinear photonics crystals, which are a big challenge if using electric field poling. The femtosecond laser poling offers an ideal technique to construct periodic ferroelectric domain devices, enabling precise control of localized domains for advanced applications in nonlinear beam shaping[35–38] and holography[39,40]. However, the generation of photon pairs from the femtosecond-fabricated QPM nonlinear structure still remains relatively unexplored. In this Letter, we use the laser-induced ferroelectric domain inversion to produce a nonlinear QPM grating in a Ti-indiffused LN waveguide. The generation of photon pairs based on the SPDC is experimentally demonstrated. Our results verify that the femtosecond poling technique provides a rapid fabrication method for QPM structures to produce quantum photon sources.

2. Device Structure Fabrication and Characteristics

In our experiment, the LN channel waveguide is fabricated by diffusing a 35-nm-thick titanium layer with a width of 3 μm on the $-Z$ surface of the crystal for a diffusion time of 22 h at a temperature of 1010°C. The refractive index contrast of the waveguide is about $\Delta n = 0.001$. The quasi-TM-polarized fundamental modes, shown in Fig. 1, are calculated using vectorial mode simulation software with the modal effective index $n_{\text{eff}} = 2.1747$ at the 812 nm wavelength and $n_{\text{eff}} = 2.3244$ at the 406 nm wavelength.

The experimental setup for the periodic inversion of ferroelectric domains is shown in Fig. 2(a). The laser (central wavelength at 800 nm, pulse width 180 fs, repetition rate 76 MHz, and single pulse energy up to 5 nJ) for domain inversion of the waveguide is generated by a femtosecond oscillator (MIRA, Coherent). The diameter of the focus spot on the crystal surface is about 1 μm by using a 40× microscope objective (NA = 0.65). The average scan speed of the focal spot of the laser beam is about $v = 10\,\mu\text{m/s}$ through the waveguide from the $-Z$ toward the Z-surface. We use an automatic shutter to block the laser beam when the sample moved to the next region of domain inversion. A typical optical image of the fabricated two-dimensional (2D) ferroelectric domain pattern after 5 min etching in hydrofluoric (HF) acid is shown in Fig. 2(b). The average QPM

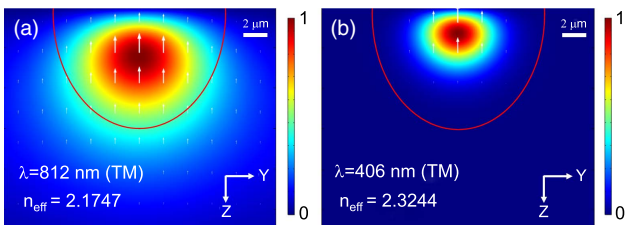

Fig. 1. Simulated mode profiles of the quasi-TM-polarized mode (a) at 812 nm for the downconverted photons and (b) at 406 nm for the pump. The scale bar is 2 μm.

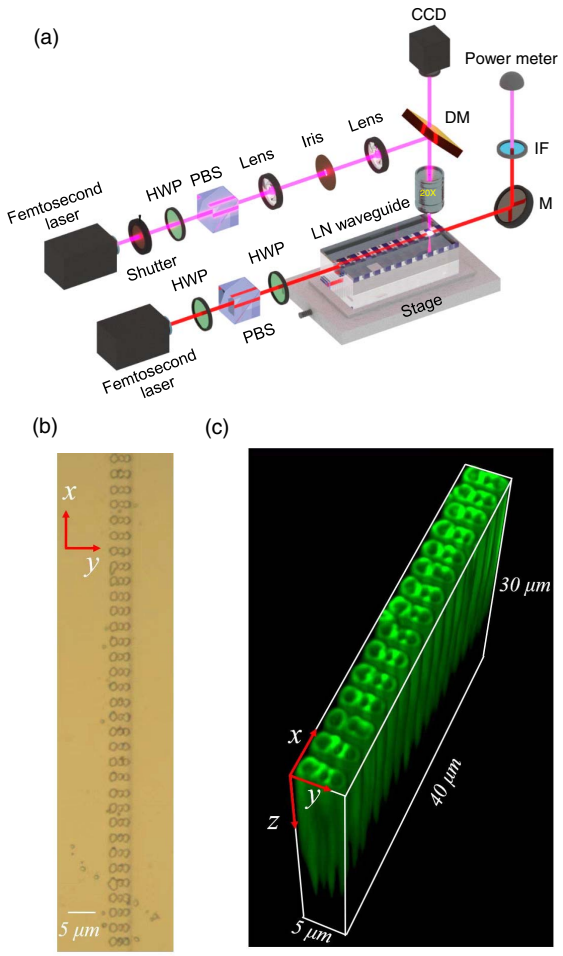

Fig. 2. (a) Experimental setup for femtosecond laser direct writing ferroelectric domain patterns in the Ti-indiffused LN channel waveguide. HWP, half-wave plate; PBS, polarizing beam splitter; DM, dichroic mirror; IF, interference filter. (b) Optical microscopic image of the 2D optically poled domain pattern with the period of 2.74 μm in the x direction and 1.15 μm in the y direction. The inverted domains are visible as small circles. (c) 3D profiles of the inverted domains obtained by Cerenkov second-harmonic microscopy.

period is $\Lambda = 2.74\,\mu\text{m}$ along the x axis and $\Lambda = 1.15\,\mu\text{m}$ along the y axis. Cerenkov second-harmonic microscopy[16,17] is used to visualize the 3D domain pattern, as shown in Fig. 2(c). The inverted domains are extended as deep as 28 μm below the surface for good overlapping between the waveguide modes of fundamental and second-harmonic.

An optimal quantum source should be able to produce a large number of photon pairs, which is determined by the nonlinear conversion efficiency of the periodically poled waveguide. For this reason, it is crucial to characterize both the propagation losses of light and nonlinear conversion efficiency to optimize the parameters for the SPDC. We will use classical characterization of the device to predict quantum behavior because the generation and detection of classical light are easier than for quantum light. First we study the reverse process of parametric downconversion (PDC), that is, second-harmonic generation (SHG). We use the microscopic objective of NA = 0.16 to focus

the 812 nm laser beam from the femtosecond oscillator (Chameleon by Coherent, pulse width of 140 fs, repetition rate of 80 MHz) into the waveguide and collect the output second harmonic using the microscope objective of NA = 0.2. The measured far-field intensity distributions of the fundamental and second-harmonic light after passing through the QPM waveguide, as shown in Figs. 3(a) and 3(b), are in good agreement with the theoretical simulation results in Fig. 1. The asymmetry of the mode sizes is consistent with typical Ti-indiffused LN waveguides. The measured spectra of the fundamental and second-harmonic waves are shown in Figs. 3(c) and 3(d), respectively. The output power of the second-harmonic wave varies with the polarization of the fundamental wave, as shown in Fig. 3(e). Its maximum value is obtained when the input polarization is parallel to the z axis of the LN waveguide (i.e., TM mode). We control the temperature to optimize the frequency-doubling process and the maximal conversion efficiency occurs at 30°C, as shown in Fig. 3(f). The propagation loss of the waveguide is measured to be about 0.1 dB/cm at the fundamental wavelength. A second-harmonic power of 4.4 mW is obtained for input power of 40 mW (peak power is 3.6 kW), and the conversion efficiency is 10.1%. This means that the device is capable of efficient photon-pair generation in the quantum domain. Thus we adopt this phase-matching condition for the production of degenerate heralded single photons.

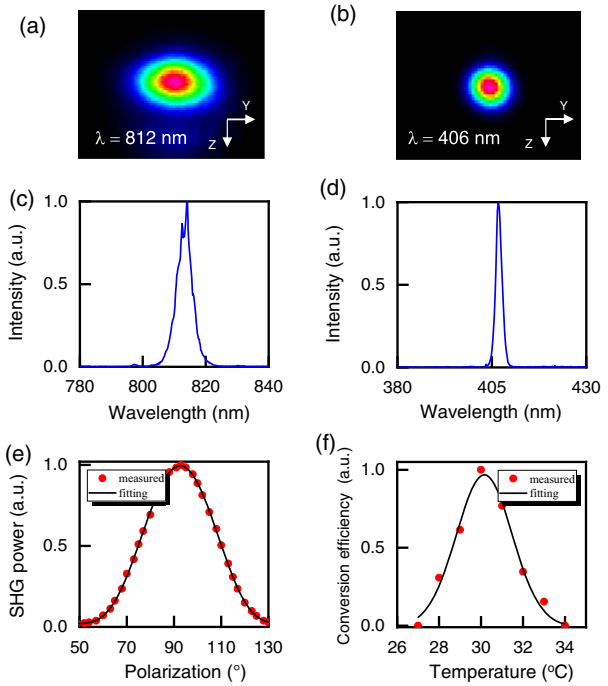

Fig. 3. Measured output intensity distribution of (a) the fundamental and (b) the second-harmonic waves in the far field; spectrum for (c) the fundamental and (d) the second-harmonic waves; (e) normalized output power of the second harmonic versus the input polarization of the fundamental wave at temperature 30°C; (f) normalized conversion efficiency of second harmonic versus the quasi-phase-matching temperature.

3. Experimental Results

The photons produced by the SPDC are measured to characterize the performance of our periodically poled LN waveguide. The experimental setup for the quantum measurements is shown in Fig. 4(a). The phase-matching condition for the SPDC was already obtained from the SHG measurements before. A 406 nm pump is generated from the SHG of the 812 nm femtosecond laser (Chameleon, Coherent) using the BBO crystal. We use two short-pass filters (Thorlabs FESH0450) and a bandpass filter (10 nm bandwidth centered 405 nm) to block the 812 nm photons. The device temperature is stabilized at 30°C. We use a polarization controller to adjust the polarization of the pump to the TM mode, which is required for Type-0 SPDC. Then, the microscopic objective (C280TMD-A) is used to focus the 406 nm laser beam into the 10 mm LN waveguide poled by the femtosecond laser, and the emitted photons are collected using the microscope objective (RMS 4X-PF). The generated signal and idler photons at 812 nm with the same vertical polarization are separated by a 50:50 fiber coupler and detected by single-photon detectors with detection efficiencies of 80%. In order to measure only the downconverted photon pairs, the emerging photons from the waveguide pass through two long-pass filters (FELH0700) and a bandpass filter (10 nm bandwidth centered at 810 nm) for blocking the 406 nm photons.

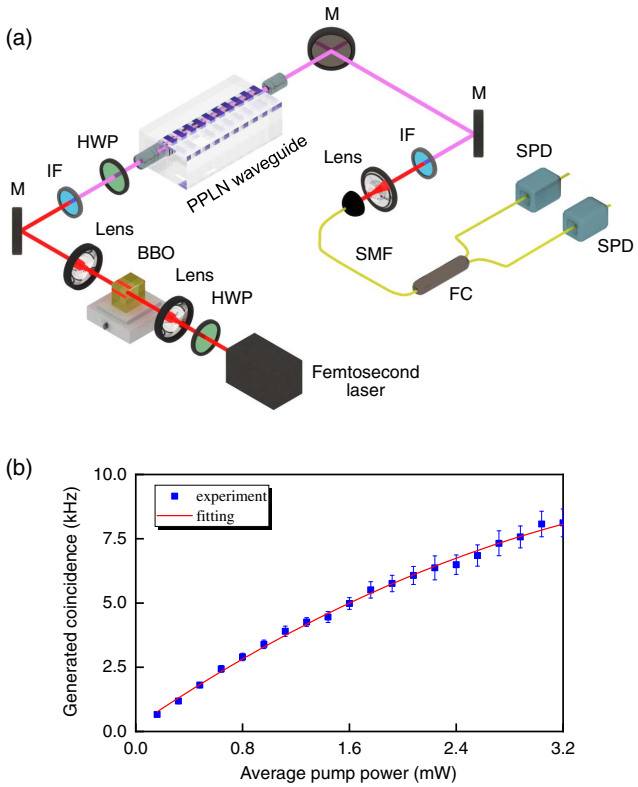

Fig. 4. (a) Schematic of the experimental setup used for photon-pair measurements. SMF, single-mode fiber; FC, fiber coupler; SPD, single-photon detector; M, mirror. (b) The coincidence of photon pairs varies with the average pump power.

The coincidence rate C_t of photon pairs depends strongly on the detector efficiency, coupling loss, and insertion losses associated with the filters used in the experiment. We focus on the generated coincidence rate $C_g = C_t/\eta_s\eta_i$ at the output of the LN waveguide, where η_s and η_i are the total collection efficiencies of the signal and idler arms, respectively, from the output of the waveguide to the detector in each path. η_s and η_i are calculated to be 0.18. Therefore, we realize the generated coincidence rate, C_g of ~8000 counts per second at the maximum average pump power of 3.2 mW (peak power is 2.9 kW). The photon generation rate can be further improved if the femtosecond laser direct-writing technique is applied to the thin-film PPLN waveguide[26] or microring resonator[21], which is beneficial for the on-chip quantum source in the future. In addition, the femtosecond laser also can be applied to fabricatation of 3D domain structures, which can increase the dimensionality and quantity of orbital angular momentum entangled states simultaneously[41].

4. Conclusion

In conclusion, we have demonstrated all-optical fabrication of QPM structures in Ti-indiffused LN waveguide using a femtosecond laser, which is a one-step process without masking procedure. The proposed scheme is efficient enough to produce correlated photon pairs based on the SPDC. The generated coincidence rate can reach ~8000 counts per second for an average pump power of 3.2 mW. Our results indicate that the femtosecond laser poling provides a powerful and flexible platform for fabricating periodic ferroelectric domains, which will benefit quantum photonic applications. It is anticipated that the manipulations of complex quantum states will be available by employing the femtosecond laser poling to control the 3D ferroelectric domains.

Acknowledgement

This work was supported financially by the National Key R&D Program of China (Nos. 2019YFA0705000, 2017YFA0303800, 2017YFA0303700, 2019YFA0308700, and 2020YFA0309500) and the National Natural Science Foundation of China (Nos. 12074197, 12074196, 11774183, and 11922406). The authors would like to thank the support from the Collaborative Innovation Center of Extreme Optics.

†These authors contributed equally to this work.

References

1. S. Pirandola, U. L. Andersen, L. Banchi, M. Berta, D. Bunandar, R. Colbeck, D. Englund, T. Gehring, C. Lupo, C. Ottaviani, J. L. Pereira, M. Razavi, J. Shamsul Shaari, M. Tomamichel, V. C. Usenko, G. Vallone, P. Villoresi, and P. Wallden, "Advances in quantum cryptography," Adv. Opt. Photonics **12**, 1012 (2020).
2. J. Yin, Y.-H. Li, S.-K. Liao, M. Yang, Y. Cao, L. Zhang, J.-G. Ren, W.-Q. Cai, W.-Y. Liu, S.-L. Li, R. Shu, Y.-M. Huang, L. Deng, L. Li, Q. Zhang, N.-L. Liu, Y.-A. Chen, C.-Y. Lu, X.-B. Wang, F. Xu, J.-Y. Wang, C.-Z. Peng, A. K. Ekert, and J.-W. Pan, "Entanglement-based secure quantum cryptography over 1,120 kilometres," Nature **582**, 501 (2020).
3. J.-Y. Hu, B. Yu, M.-Y. Jing, L.-T. Xiao, S.-T. Jia, G.-Q. Qin, and G.-L. Long, "Experimental quantum secure direct communication with single photons," Light Sci. Appl. **5**, e16144 (2016).
4. J. M. Arrazola, V. Bergholm, K. Bradler, T. R. Bromley, M. J. Collins, I. Dhand, A. Fumagalli, T. Gerrits, A. Goussev, L. G. Helt, J. Hundal, T. Isacsson, R. B. Israel, J. Izaac, S. Jahangiri, R. Janik, N. Killoran, S. P. Kumar, J. Lavoie, A. E. Lita, D. H. Mahler, M. Menotti, B. Morrison, S. W. Nam, L. Neuhaus, H. Y. Qi, N. Quesada, A. Repingon, K. K. Sabapathy, M. Schuld, D. Su, J. Swinarton, A. Száva, K. Tan, P. Tan, V. D. Vaidya, Z. Vernon, Z. Zabaneh, and Y. Zhang, "Quantum circuits with many photons on a programmable nanophotonic chip," Nature **591**, 54 (2021).
5. J. B. Spring, B. J. Metcalf, P. C. Humphreys, W. S. Kolthammer, X.-M. Jin, M. Barbieri, A. Datta, N. Thomas-Peter, N. K. Langford, D. Kundys, J. C. Gates, B. J. Smith, P. G. R. Smith, and I. A. Walmsley, "Boson sampling on a photonic chip," Science **339**, 798 (2012).
6. H.-S. Zhong, H. Wang, Y.-H. Deng, H.-S. Zhong, H. Wang, Y.-H. Deng, M.-C. Chen, L.-C. Peng, Y.-H. Luo, J. Qin, D. Wu, X. Ding, Y. Hu, P. Hu, X.-Y. Yang, W.-J. Zhang, H. Li, Y. Li, X. Jiang, L. Gan, G. Yang, L. You, Z. Wang, L. Li, N.-L. Liu, C.-Y. Lu, and J.-W. Pan, "Quantum computational advantage using photons," Science **370**, 1460 (2020).
7. M. A. Taylor and W. P. Bowen, "Quantum metrology and its application in biology," Phys. Rep. **615**, 1 (2011).
8. V. Giovannetti, S. Lloyd, and L. Maccone, "Advances in quantum metrology," Nat. Photonics **5**, 222 (2011).
9. J.-W. Wang, F. Sciarrino, A. Laing, and M. G. Thompson, "Integrated photonic quantum technologies," Nat. Photonics **14**, 273 (2020).
10. L.-L. Lu, X.-D. Zheng, Y.-Q. Lu, S.-N. Zhu, and X.-S. Ma, "Advances in chip-scale quantum photonic technologies," Adv. Mater. Technol. **4**, 2100068 (2021).
11. J. Kim, S. Aghaeimeibodi, J. Carolan, D. Englund, and E. Waks, "Hybrid integration methods for on-chip quantum photonics," Appl. Phys. Lett. **7**, 291 (2020).
12. C. P. Dietrich, A. Fiore, M. G. Thompson, M. Kamp, and S. Hofling, "GaAs integrated quantum photonics: towards compact and multi-functional quantum photonic integrated circuits," Laser Photonics Rev. **10**, 870 (2016).
13. L.-T. Feng, M. Zhang, J.-W. Wang, X.-Q. Zhou, X.-G. Qiang, G.-C. Guo, and X. Ren, "Silicon photonic devices for scalable quantum information applications," Photonics Res. **10**, A135 (2022).
14. P. Senellart, G. Solomon, and A. White, "High-performance semiconductor quantum-dot single-photon sources," Nat. Nanotechnol. **12**, 1026 (2017).
15. Y.-C. Wang, K. D. Jons, and Z.-P. Sun, "Integrated photon-pair sources with nonlinear optics," Appl. Phys. Rev. **8**, 11314 (2021).
16. L. Caspani, C.-L. Xiong, B. J. Eggleton, D. Bajoni, M. Liscidini, M. Galli, R. Morandotti, and D. J. Moss, "Integrated sources of photon quantum states based on nonlinear optics," Light Sci. Appl. **6**, e17100 (2017).
17. A. Orieux, M. A. M. Versteegh, K. D. Jons, and S. Ducci, "Semiconductor devices for entangled photon pair generation: a review," Rep. Prog. Phys. **80**, 76001 (2017).
18. X.-Y. Lu, S. Rogers, T. Gerrits, W. C. Jiang, S. Nam, and Q. Lin, "Heralding single photons from a high-q silicon microdisk," Optica **3**, 1331 (2016).
19. Z.-H. Yin, K. Sugiura, H. Takashima, R. Okamoto, F. Qiu, S. Yokoyama, and S. Takeuchi, "Frequency correlated photon generation at telecom band using silicon nitride ring cavities," Opt. Express **29**, 4821 (2021).
20. S. Castelletto, A. Peruzzo, C. Bonato, B. C. Johnson, M. Radulaski, H.-Y. Ou, F. Kaiser, and J. Wrachtrup, "Silicon carbide photonics bridging quantum technology," ACS Photonics **9**, 1434 (2022).
21. Z. Ma, J. Chen, Z. Li, C. Tang, Y. M. Sua, H. Fan, and Y.-P. Huang, "Ultrabright quantum photon sources on chip," Phys. Rev. Lett. **125**, 263602 (2020).
22. Z.-D. Xie, T. Zhong, S. Shrestha, X.-A. Xu, J.-L. Liang, Y.-X. Gong, J. C. Bienfang, A. Restelli, J. H. Shapiro, F. N. C. Wong, and C. W. Wong, "Harnessing high-dimensional hyperentanglement through a biphoton frequency comb," Nat. Photonics **9**, 536 (2015).
23. S. Bogdanov, M. Y. Shalaginov, A. Boltasseva, and V. M. Shalaev, "Material platforms for integrated quantum photonics," Opt. Mater. Express **7**, 111 (2017).

24. B.-Y. Xu, L.-K. Chen, J.-T. Lin, L.-T. Feng, R. Niu, Z.-Y. Zhou, R.-H. Gao, C.-H. Dong, G.-C. Guo, Q.-H. Gong, Y. Cheng, Y.-F. Xiao, and X.-F. Ren, "Spectrally multiplexed and bright entangled photon pairs in a lithium niobate microresonator," Sci. China Phys. Mech. Astron. **65**, 294262 (2022).
25. T. Wang, P. Chen, C. Xu, Y. Zhang, D.-Z. Wei, X.-P. Hu, G. Zhao, M. Xiao, and S. Zhu, "Periodically poled $LiNbO_3$ crystals from 1D and 2D to 3D," Sci. China Technol. **63**, 1110 (2020).
26. J. Zhao, C.-X. Ma, M. Rusing, and S. Mookherjea, "High quality entangled photon pair generation in periodically poled thin-film lithium niobate waveguides," Phys. Rev. Lett. **124**, 163603 (2020).
27. H. Jin, F. M. Liu, P. Xu, J. L. Xia, M. L. Zhong, Y. Yuan, J. W. Zhou, Y. X. Gong, W. Wang, and S. N. Zhu, "On-chip generation and manipulation of entangled photons based on reconfigurable lithium-niobate waveguide circuits," Phys. Rev. Lett. **113**, 103601 (2014).
28. M. B. Nasr, S. Carrasco, B. E. A. Saleh, A. V. Sergienko, M. C. Teich, J. P. Torres, L. Torner, D. S. Hum, and M. M. Fejer, "Ultrabroadband biphotons generated via chirped quasi-phase-matched optical parametric down-conversion," Phys. Rev. Lett. **100**, 183601 (2008).
29. A. Tanaka, R. Okamoto, H. Lim, S. Subashchandran, M. Okano, L.-B. Zhang, L. Kang, J. Chen, P. Wu, T. Hirohata, S. Kurimura, and S. Takeuchi, "Noncollinear parametric fluorescence by chirped quasi-phase matching for monocycle temporal entanglement," Opt. Express **20**, 25228 (2012).
30. D. Wei, C. Wang, H. Wang, X. Hu, D. Wei, X. Fang, Y. Zhang, D. Wu, Y. Hu, J. Li, S. Zhu, and M. Xiao, "Experimental demonstration of a three dimensional lithium niobate nonlinear photonic crystal," Nat. Photonics **12**, 596 (2018).
31. T.-X. Xu, K. Switkowski, X. Chen, S. Liu, K. Koynov, H.-H. Yu, H. Zhang, J. Wang, Y. Sheng, and W. Krolikowski, "Three-dimensional nonlinear photonic crystal in ferroelectric barium calcium titanate," Nat. Photonics **12**, 591 (2018).
32. Y. Zhang, Y. Sheng, S.-N. Zhu, M. Xiao, and W. Krolikowski, "Nonlinear photonic crystals: from 2D to 3D," Optica **8**, 372 (2021).
33. B. Zhang, L. Wang, and F. Chen, "Recent advances in femtosecond laser processing of $LiNbO_3$ crystals for photonic applications," Laser Photonics Rev. **14**, 1900407 (2020).
34. X.-Y. Xu, T.-X. Wang, P.-C. Chen, C. Zhou, J.-N. Ma, D.-Z. Wei, H. Wang, B. Niu, X. Fang, D. Wu, S. Zhu, M. Gu, M. Xiao, and Y. Zhang, "Femtosecond laser writing of lithium niobate ferroelectric nanodomains," Nature **609**, 496 (2022).
35. X.-P. Hu, Y. Zhang, and S.-N. Zhu, "Nonlinear beam shaping in domain engineered ferroelectric crystals," Adv. Mater. **32**, 1903775 (2019).
36. D.-Z. Wei, C.-W. Wang, X.-Y. Xu, H.-J. Wang, Y.-L. Hu, P.-C. Chen, J. Li, Y. Zhu, C. Xin, X. Hu, Y. Zhang, D. Wu, J. Chu, S. Zhu, and M. Xiao, "Efficient nonlinear beam shaping in three dimensional lithium niobate nonlinear photonic crystals," Nat. Commun. **10**, 4193 (2019).
37. S. Liu, K. Switkowski, C.-L. Xu, J. Tian, B.-X. Wang, P.-X. Lu, W. Krolikowski, and Y. Sheng, "Nonlinear wavefront shaping with optically induced three-dimensional nonlinear photonic crystals," Nat. Commun. **10**, 3208 (2019).
38. B.-X. Wang, S. Liu, T.-X. Xu, R.-W. Zhao, P.-X. Lu, W. Krolikowski, and Y. Sheng, "Nonlinear talbot self-healing in periodically poled $LiNbO_3$ crystal," Opt. Express **19**, 60011 (2021).
39. S. Liu, L. M. Mazur, W. Krolikowski, and Y. Sheng, "Nonlinear volume holography in 3D nonlinear photonic crystals," Laser Photonics Rev. **14**, 2000224 (2020).
40. P.-C. Chen, C.-W. Wang, D.-Z. Wei, Y.-L. Hu, X.-Y. Xu, J.-W. Li, D. Wu, J. Ma, S. Ji, L. Zhang, L. Xu, T. Wang, C. Xu, J. Chu, S. Zhu, M. Xiao, and Y. Zhang, "Quasi-phase-matching-division multiplexing holography in a three-dimensional nonlinear photonic crystal," Light Sci. Appl. **10**, 146 (2021).
41. Q. Yu, C. Xu, S.-X. Chen, P.-C. Chen, S.-W. Nie, S.-J. Ke, D. Wei, M. Xiao, and Y. Zhang, "Manipulating orbital angular momentum entanglement in three-dimensional spiral nonlinear photonic crystals," Photonics **9**, 504 (2022).